

Research Paper

Dose-dependent Effects of Strontium Ranelate on Ovariectomy Rat Bone Marrow Mesenchymal Stem Cells and Human Umbilical Vein Endothelial Cells

Xiaojing Guo^{1*}, Silong Wei^{2*}, Mengmeng Lu¹, Zhengwei Shao¹, Jiayu Lu¹, Lunguo Xia², Kaili Lin^{3✉}, Derong Zou^{1✉}

1. Department of Stomatology, Shanghai Jiao Tong University Affiliated Sixth People's Hospital, Shanghai, 200233, China;
2. Department of Oral and Craniomaxillofacial Sciences, Shanghai Ninth People's Hospital Affiliated to Shanghai Jiao Tong University School of Medicine, Shanghai 200011, China;
3. School & Hospital of Stomatology, Tongji University, Shanghai Engineering Research Center of Tooth Restoration and Regeneration, Shanghai 200072, China.

*First author and co-first author.

✉ Corresponding authors: Derong Zou. Phone number: +86 18930177322; Email address: drzou@sjtu.edu.cn. Or Kaili Lin. Phone number: +86-21-56722215; Email address: linkaili@tongji.edu.cn.

© Ivyspring International Publisher. Reproduction is permitted for personal, noncommercial use, provided that the article is in whole, unmodified, and properly cited. See <http://ivyspring.com/terms> for terms and conditions.

Received: 2016.06.16; Accepted: 2016.09.26; Published: 2016.11.25

Abstract

In clinic, strontium ranelate (SrR) is a useful drug to treat osteoporosis by orally taken method, but some side effect appeared in recent years. The aim of this study is to evaluate the effectiveness and safety of SrR on cells by direct application, to study the possibility of local application of this drug. Qualitative ALP staining, quantitative ALP activity assay, alizarin red staining, realtime PCR and westernblot assay were used to evaluate the osteogenesis ability of SrR under normal or osteogenic induction environment of ovariectomy bone marrow mesenchymal stem cells (OVX-BMSCs). The angiogenesis ability of SrR was studied by immunofluorescence staining of CD31 and vWF of OVX-BMSCs under angiogenesis induction environment, transwell, tubeformation and realtime PCR assay of HUVECs. Signaling pathway of PI3K/AKT/mTOR was also studied. The result demonstrated that SrR could enhance proliferation and osteogenic differentiation of OVX-BMSCs. The osteogenesis effect of SrR has been proved by the better performed of ALP activity, alizarin red staining and the remarkable up-regulation of ALP, Col-I, Runx2, OCN, BMP-2, BSP, OPG of the OVX-BMSCs, and reduction of RANKL. In addition, SrR promotes angiogenesis differentiation of both OVX-BMSCs and HUVECs. Higher intensity of immunostaining of CD31 and vWF, better result of transwell and tubeformation assay could be observed in SrR treated group, and increasing mRNA levels of VEGF and Ang-I in the OVX-BMSCs, VEGF in HUVECs were learnt. Signaling pathway assay showed that PI3K/AKT/mTOR signaling pathway was involved in this SrR triggered angiogenesis procedure. The thrombosis marker ET-I, PAI-I and t-PA were up-regulated, but no significant differences for low concentration (<0.5mM). The concentration between 0.25-0.5mM may be more appropriate for local application, and locally application of SrR could be considered as a promising way for bone regeneration.

Key words: Strontium Ranelate, OVX-BMSCs, HUVECs, Osteogenesis, Angiogenesis.

Introduction

Osteoporosis is a metabolic bone disorder characterized by a high bone turnover, low bone mass, destruction of bone microstructure, and

increased risk of bone fragility and fractures[1]. In patients with osteoporosis, osteogenesis regression and osteoclasts enhancement occurs, also weakening

angiogenesis exists, resulting in deteriorated bone microstructure[2].

Strontium ranelate (SrR) is an anti-osteoporosis drug used for postmenopausal osteoporosis women and man for more than 10 years[3]. Randomized controlled clinical trials showed that SrR significantly improved bone mineral density and bone quality of the patients, and markedly reduce risk of spine or hip fractures[4-8]. In the patients with osteoporosis especially postmenopausal women with osteoporosis, a follow-up study for 10 years showed that SrR brought a long-term clinical benefit with a high level of safety[2,9].

The molecular structure of SrR contains two non-radioactive strontium and a ranelate acid, displaying a dual regulatory effect of bone formation promotion and bone resorption inhibition[10]. For bone formation, SrR promotes proliferation and osteogenic differentiation of mesenchymal stem cells (MSCs) or osteoblast cells, including up-regulated the protein expression levels of early and middle stage osteogenic marker such as ALP, Col-I, Runx2, OCN, and BSP, thereby accelerating matrix mineralization and nodule formation[11]. The underlying mechanism of SrR osteogenesis is complicated. It has been confirmed that several signal pathways are involved in this event. For the similar atomic and ionic properties of Sr^{2+} to Ca^{2+} , SrR can bind with calcium-sensing receptor (CaSR), and promote osteogenesis via MAPK/Erk 1/2 signaling pathways[12,13], PI3K/AKT signaling pathways[14]. Besides CaSR, other sensing receptors also react to SrR. The study of Olivia demonstrated that Calcineurin/NFATc1 pathway, and canonical or non-canonical Wnt pathway are involved in SrR-induced osteoblast differentiation[15]. Moreover, Ras/MAPK[16], MAPK/p38[17], BMP-2/Smad and hedgehog signaling pathways[18] governing osteoblast differentiation are also activated. In addition, SrR has some other functions that have been proved, such as its positive effect on Ca^{2+} permeable nonselective cation channel to elevate Ca^{2+} level in cells[12], and up-regulate sclerostin which plays an essential role in bone remodeling[19]. On the other hand, SrR decreases bone resorption by inhibiting differentiation and increasing apoptosis of osteoclast progenitors[9], in which RANK/RANKL/OPG system is involved as the key mechanism. Further, this effect was only produced by SrR and could not be replaced by strontium chloride or sodium ranelate, those used as replacement of SrR to gain a higher solution[20].

However, orally taken SrR will waste the ranelate due to the barrier of gastrointestinal mucosa[4], but it still used as the standard route of

administration in clinical application. Orally taken method can reach a serum level of 0.12mM after 3 years of regular taken of SrR 2g per day[21], that is lower than the effective dosage reported previously[9,11,22]. Though Sr^{2+} level is higher in bone tissue than in serum, no data could be approved. Moreover, the side effect of SrR including gastrointestinal dysfunction, headache, dermatitis, eczema etc. may directly relate to the orally taken method and the serum drug level. Recently, an increased risk of venous thromboembolism or myocardial infarction in patients treated with SrR has been officially warned by the European Medicines Agency European Medicine Agency (EMA). While, no experimental evidence has been found, and some retrospective studies demonstrated that the casual relation between SrR treatment and cardiovascular event is still remained uncertain [2,23,24]. For the thrombosis effect of SrR has been observed in clinical application, a safer and more effective way of SrR application is needed.

Local administration of SrR on bone tissue regeneration may have some advantages theoretically. First, it avoids the gastrointestinal mucosa that the whole molecular of SrR could goes into the target area, that may perform more effectively; Second, the high attraction of bone tissue will reduce the disassociated SrR to go into cardiovascular system which may reduce the risk of cardiovascular event, and keep a relatively high concentration of SrR in bone tissue. Third, some side effects could be avoided, such as discomfort of gastrointestinal system. Fourth, the lower successful rate of oral implant treatment for osteoporosis patients may attribute to the delayed bone integration, but it still can reach the final goal of sufficient osseointegration[25]. Locally application drug could accelerate this procedure to reach the sufficient osseointegration earlier, which is more time saving and effective than osteoporosis treatment. Tian and Nair uploaded SrR on some biomaterial to achieve the local delivery of SrR, and all got a good result of bone regeneration[26,27]. Nevertheless, questions about the effectiveness and safety of SrR local delivery have been raised.

The aim of present study is to evaluate the effectiveness and safety of SrR on cells directly. An intact compound of SrR was used, and quite large ranges of concentration were studied to get more detailed information. OVX-BMSCs were used as a cellular model with insufficient osteogenic ability, and HUVECs to study the drug effect on vascular tissue. The osteogenesis ability and angiogenesis ability of OVX-BMSCs or HUVECs were tested by different methods, and also the gene expressions related to

thrombosis effect were analyzed.

Materials and methods

Isolation and culture of rat-derived OVX-BMSCs

All of the animal experiments were performed in accordance of NIH guidelines, and approved by the Animal Research Committee of the Shanghai Jiao Tong University Affiliated Sixth People's Hospital (Shanghai, China). Female healthy Sprague-Dawley (SD) rats of 3-month-old were housed in individual cages in an animal room maintained at 22°C with a 12h-light/dark cycle. The rats were given free access to water and food. All of the animals received an ovariectomy surgery through two dorsal incisions [28]. Three months after the surgery, the rats were sacrificed by an overdose of pentobarbital sodium. Bilateral femurs were collected and all soft tissues were removed under an aseptic condition. Metaphyses from both ends of the femur were cut off and the marrow was flushed out with 10 ml of Dulbecco's Modified Eagle's medium (DMEM) (Gibco, USA) supplemented with 10% fetal bovine serum (Gibco, USA) and antibiotics containing 100U/ml penicillin and 100U/ml streptomycin. The cells were seeded in 10 cm-diameter plates and cultured at 37°C in a 5% CO₂ incubator. The culture medium was replaced every 2-3 days. The cells were passaged when they reached a confluence of 80%. OVX-BMSCs in passage 2-4 were used in this study.

OVX-BMSCs identification

Immunofluorescence staining was used for OVX-BMSCs identification, according to the minimal criteria to define MSC released by the Mesenchymal and Tissue Stem Cell Committee of the International Society for Cell Therapy [29]. For OVX-BMSCs share the same surface marker of normal BMSCs, CD44, CD90, and CD105 were chosen as positive markers, while CD34 and CD45 as negative markers. OVX-BMSCs were seeded in 24-well plate at a density of 8×10^4 /well, and incubated with anti-bodies after fixed with formalin. CD44(1:40, R&D Systems, USA), CD90(1:200, abcam, UK), CD105(1:40, R&D Systems, USA), CD34(1:100, abcam, UK) and CD45(1:200, NOVUS, USA) antibodies were used as primary anti-bodies, and Alexa Fluor® 488 Donkey Anti-goat/rat/mouse IgG(Invitrogen, USA) were used as secondary anti-bodies. Cell nuclei were stained with 4' 6-diamidino-2-phenylindole (DAPI; Vector Labs, USA). Microscope (Leica, DMI 3000B, Germany) of 100 magnifications was used for photograph.

Preparation of SrR

51.35 mg of SrR (Sigma-Aldrich, USA) were dissolved in 50 ml of high-glucose DMEM supplemented with 10% FBS, 100U/ml penicillin, and 100U/ml streptomycin at 37°C for 5-10 min until it totally dissolved, then filtered by a sheet of 0.22µm filter membrane (Millipore, Germany). SrR was prepared to a solution to reach a final concentration of 2.0mM, and then diluted into various concentrations of 1.0, 0.5, 0.25 and 0.125mM.

Cell proliferation assay of OVX-BMSCs

The cell proliferation of OVX-BMSCs in response to different concentrations of SrR was measured by MTT assay. OVX-BMSCs were seeded in 96-well plates (3×10^3 cells/well), and then treated with different concentrations of SrR (0, 0.125, 0.25, 0.5, 1.0, 2.0 and 4.0mM, while 4.0mM were turbid liquid) respectively for 1, 3, 5, 7d. 10µl of MTT solution (5mg/ml) was added in the wells and co-incubated in dark at 37°C, 5%CO₂ for 4h. Then, 100µl of DMSO solution was added to dissolve the formazana. The cell viability was assessed by measuring the optical density (OD) at 570nm in a full spectrum microplate spectrophotometer (Bio-Tek, USA). The control wells also served. Data from triplicate samples were averaged.

ALP activity assay of OVX-BMSCs

To determine the early differentiation of the OVX-BMSCs stimulated by SrR, ALP staining and ALP activity were assayed. For ALP staining, the cells were cultured in a 24-well plate (4×10^4 /well) with different concentrations of SrR (0, 0.125, 0.25, 0.5, 1.0, and 2.0mM). An ALP staining kit (Beyotime, China) was used 7 days after the culture. Briefly, after formalin fixation for 10min, BCIP/NBT working solution were added into each well and incubated in dark room temperature for 30min. Then rinsed with distilled water twice and counterstained by Neutral red (Beyotime, China) for 5min, photographed by microscope.

ALP activity was determined in 6-well plates (density of 1×10^5 /well) treated with different concentrations of SrR, and an alkaline phosphatase assay kit (Nanjing Jian Cheng, China) was used at day 4, 7 and 10. Cells were rinsed with cold PBS for three times, and lysed by RIPA (Sigma, USA) on ice. Total protein concentration was determined by BCA protein assay kit (Beyotime, China). The optical density (OD) of ALP protein was measured at 520nm in accordance with the instructions of the manufacturer's instruction. ALP activity was calculated by ALP level normalized to the total protein.

Osteogenesis assay of OVX-BMSCs under osteogenic induction

To fully understand the drug effect, the osteogenesis ability of OVX-BMSCs using osteogenic induction cultural medium was tested. The osteogenic induction medium contained dexamethasone, β -glycerophosphate and ascorbic acid, and the cultural medium was changed every 3 days.

Qualitative ALP staining was performed at day 7, while quantitative ALP activity assay at day 4, 7 and 10. Alizarin red staining (Cyagen Biosciences, USA) was conducted following the manufacturer's instruction at day 21. Briefly, cells were stained by Alizarin red S for 5min after fixed by formalin, washed by PBS for two times and photograph by microscope. Then quantitative data were got by dissolving the staining with 500 μ l cetylpyridinium and absorbance of the liquid was measured at 578nm. Realtime-PCR assay at day 4 and 7 were also studied.

Angiogenesis ability assay of OVX-BMSCs under angiogenesis induction

VEGF at 10ng/ml and bFGF at 2ng/ml were added into the cultural medium for vessel endothelial cells induction, in addition with the supplying of different concentrations of SrR (0.25, 0.5 and 1.0mM). Cultural medium was changed every two days.

After 14 days of induction, the differentiation degrees of OVX-BMSCs were evaluated by LDL uptake assay and immunofluorescence staining. For LDL uptake assay, OVX-BMSCs or HUVECs (as positive control) were seeded in 24-well plate at a density of 8×10^4 /well, and incubated in cultural medium added with 20 μ g/ml Acetylated Low Density Lipoprotein labeled with 1,1'-dioctadecyl - 3,3,3',3'-tetramethyl-indocarbocyanine perchlorate (Dli-Ac-LDL, Luwen Biotechnology, China) for 4h at 37°C. Then, washed by PBS for three times, and visualized by fluorescence microscopy.

For immunofluorescence staining, OVX-BMSCs or HUVECs were seeded in 24-well plate at a density of 8×10^4 /well, and incubated with anti-bodies after fixed with formalin. Rabbit/Goat anti rat CD 31(1:100, proteintech, USA) and vWF (1:100, abcam, UK) were used as primary antibodies, Alexa Fluor® 488 Donkey Anti-Rabbit IgG (Invitrogen, USA) and Alexa Fluor® 555 Donkey Anti-Goat IgG (Invitrogen, USA) were used as secondary anti-bodies. Cell nuclei were stained by DAPI (Vector Labs, USA). Microscope (Leica, DMI 3000B, Germany) of 100 magnifications was used for photographing.

HUVECs culture and treatments

HUVECs were purchased from the cell bank of Chinese Academy of Sciences (Shanghai, China). SrR

treatments were performed as described previously.

Angiogenesis assay of HUVECs

The in-vitro angiogenesis assay was carried out by using transewell test and tube formation assay. The HUVECs (1×10^5 cells/ml) were treated with serum-free culture containing different concentrations of SrR for 24 hours, and seeded 200 μ l of cell solution at the upper chamber, and 500 μ l of culture medium supplemented with 10%FBS and different concentrations of SrR at the lower chamber. After incubation for 24 hours, the cells were washed with PBS and fixed with formalin. The migrated cells were stained with 0.1% crystal violet and photographed by an optical microscope. After that, the chambers were washed by 500 μ l of 33% acetic acid to dissolve the crystal violet. The absorbance was measured by using a microplate reader at 570nm.

The Matrigel (BD, USA) were used for tube formation test according to the manufacture's instructions. HUVECs (1×10^5 cells/well) in 6-well plates were treated with culture medium containing different concentrations of SrR for 48 h. 96-well plates were coated with 100 μ l Matrigel for 30min, and then the different treated HUVECs (2×10^5 cells/well) were cultured on the Matrigel for 4-12h. The cells were photographed at five random microscopic fields using an inverted light microscope (Leica DMI 3000B, Germany). Quantitative analyses were performed in accordance with the manufacturer's instructions. Tubes, loops and branching points were calculated.

Western Blotting assay

OVX-BMSCs or HUVECs were seeded in 6-well plates (2×10^5 cells/well). OVX-BMSCs were cultured in medium supplemented with 100 μ M CoCl₂ and different concentrations of SrR (0, 0.125, 0.25, 0.5, 1.0 and 2.0mM) for 48h. HUVECs were cultured in medium with SrR at 0.25mM for 0, 15, 30, 60 and 90 min. Then cells were washed by cold PBS, and lysed with RIPA for protein extraction. Total protein concentration was measured by a BCA protein assay kit.

Equal amount of protein samples were separated by 12% SDS-PAGE, and transferred to a polyvinylidene fluoride membrane. After blocking with 5% skim milk for 1h, the membrane was incubated with mouse anti-rat HIF-1 α (1:1000, CST, USA), SDF-1(1:200, Abcam, UK), VEGF (1:1000, Abcam, UK) and β -actin (1:5000, Sigma, USA) for OVX-BMSCs, rabbit anti human AKT, phosphorylated-AKT (p-AKT), mTOR, phosphorylated -mTOR (p-mTOR) (1:1000, CST, USA) for HUVECs at 4 °C overnight. Then followed by a 2h incubation with HRP-conjugated goat anti-rabbit or

rabbit anti mouse IgG (1:3000, Beyotime, China) at room temperature and washed by PBST for 3 times. Immunoreactive bands were detected by enhanced chemiluminescence (ECL) reagent (Pierce, USA), visualized by autoradiography and quantified by the Quantity One analysis system (Bio-Rad, USA). β -actin served as the internal control.

Signaling pathway inhibition assay of HUVECs

HUVECs were cultured in the medium with or without PI3K/AKT signaling pathway inhibitor LY294002 for 30min, then treated with SrR (0 or 0.25mM) for 90min. The protein expressions of p-AKT, AKT, p-mTOR, mTOR were detected by western blot assay. Moreover, tube formation assay was conducted after HUVECs treated with or without LY294002 for 30min, and incubated with SrR (0 or 0.25mM) for 6h. Microscope (Leica, DMI 3000B, Germany) of 100 magnifications was used for photograph.

Quantitative Real-time PCR assay

The OVX-BMSCs or HUVECs were cultured in 6-well plates (1×10^5 cells/well) and treated with different concentrations of SrR (0, 0.125, 0.25, 0.5, 1.0 and 2.0mM). Total RNA was extracted from the cells at different timing by using the TRIzol reagent (Ambion, USA) and used as template (2 μ g) for reverse transcription with PrimeScript RT reagent kit (TAKARA, Japan). The resultant cDNA (2 μ l) was amplified in a 20 μ l reaction system consisting of 10 μ l of SYBR Premix Ex Taq, 0.4 μ l ROX dye II, 0.8 μ l of forward and reverse primers (10 μ M each), and 6.8 μ l of ddH₂O. Primer sequences are listed in Table 1 and Table 2. Triplicate reactions were performed and the relative fold-change of gene expression was determined by normalizing to GAPDH and calculating the $2^{-\Delta\Delta CT}$ (7500 system SDS software, version 1.2.3; Applied Biosystems, USA).

Statistical Analysis

Data were expressed as mean \pm SD. The differences among groups were compared by one-way analysis of variance (ANOVA), using SPSS 21.0 software (SPSS Inc., USA). A *p* value of less than 0.05 was thought to be significant.

Results

OVX-BMSCs identification

OVX-BMSCs were isolated from the OVX rat-derived bone marrow, and identified by Immunofluorescence assay. As shown in Figure 1, the cultured cells were positively immunostained with CD44, CD90 and CD105, while negatively stained with CD45 and CD34 (Figure 1).

Table 1. Primer sequences used for the OVX-BMSCs.

Gene Target	Primers sequence (5'-3')	Product size (bp)
Col-1	Forward: GGTCCCAAAGGTGCTGATGG	182
	Reverse: GACCAGGCTCACCACGGTCT	
ALP	Forward: GTCCCAACAAGAGCCACAAT	172
	Reverse: CAACGGCAGAGCCAGGAAT	
Runx2	Forward: ATCCAGCCACCTTCACITACACC	199
	Reverse: GGGACCATTGGGAAGTATAGG	
OCN	Forward: CAGTAAGGTGGTGAATAGACTCCG	172
	Reverse: GGTGCCATAGATGCGCTTG	
BMP-2	Forward: GAAGCCAGGTGTCTCCAAGAG	122
	Reverse: GTGGATGTCCTTTACCGTCGT	
OPG	Forward: GTCCCTTGCCCTGACTACTCT	250
	Reverse: GACATCTTTTIGCAAACCGTGT	
RANKL	Forward: CCCATCGGGTCCCATAAAGTC	146
	Reverse: GCCTGAAGCAAATGTTGGCGTA	
BSP	Forward: AGAAAGAGCAGCAGCGTTGAGT	175
	Reverse: GACCTCTGAGCCITCATAGCC	
VEGF	Forward: GGCTCTGAAACCATGAACITTTCT	165
	Reverse: GCAGTAGCTGCGCTGGTAGAC	
ANG-1	Forward: GGACAGCAGGCAAACAGAGCAGC	130
	Reverse: CCACAGGCATCAAACCAACCAACC	
GAPDH	Forward: GGCAAGTTCAACGGCACAGT	76
	Reverse: GCCAGTAGACTCCACGACAT	

Table 2. Primer sequences used for the HUVECs.

Gene Target	Primers sequence (5'-3')	Product size (bp)
ET-1	Forward: CAGAGGCGATCACAGCAACCA	296
	Reverse: CAAGGAGCAGGAGCAACG	
VEGF	Forward: GAGTACCCTGATGAGATCGAGT	193
	Reverse: ATTTGTGTGCTGTAGGAAGCT	
PAI-1	Forward: TGCCTCTACTTCAACGG	307
	Reverse: GTCGGICATCCCAGGTT	
t-PA	Forward: CCAGATCGAGACTCAAAGCC	119
	Reverse: GACCCATTCCCAAAGTAGCA	
GAPDH	Forward: CGTATTGGGCGCCTGTGTAC	248
	Reverse: ACGTACTCAGCGCCAGCATCG	

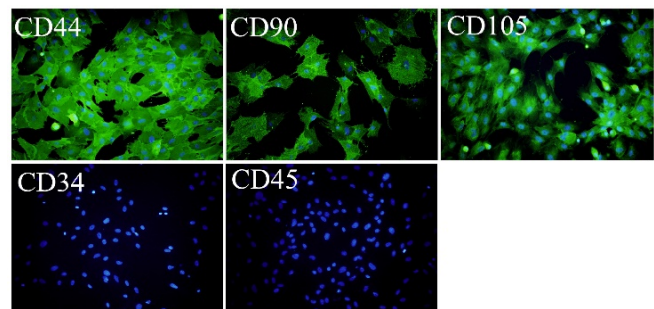


Figure 1. Immunofluorescence assay of the isolated OVX-BMSCs ($\times 100$). The cells were positively stained with CD44, CD90 and CD105, while negative stained with CD34 and CD45. The cell nucleus was stained with DAPI.

Cell proliferation assay of OVX-BMSCs

The MTT assay showed that there was no significant difference for the proliferation of the OVX-BMSCs between control group and SrR-treated

at low concentration (0.125, 0.25, 0.5 mM) at day 1, 3, and 5. At day 7, the concentration of 0.125mM and 0.25mM could significantly enhance the cell proliferation, while 0.5mM had no difference with the control group. However, the high concentration of SrR (1.0, 2.0 and 4.0mM) could significantly suppress the cell proliferation at day 3, 5 and 7 ($p < 0.05$) (Figure 2).

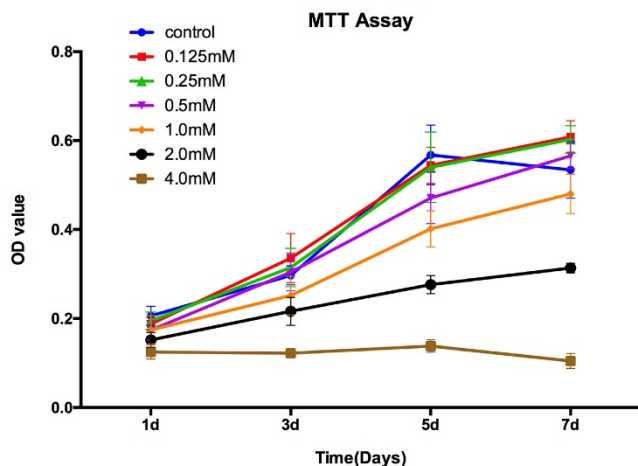


Figure 2. MTT assay for OVX-BMSCs treated with different concentrations of SrR. The experiment was repeated for at least 3 times, and the data were expressed as mean \pm SD. The OD 570 values were measured at the specific time points to draw curves.

Osteogenesis assay of OVX-BMSCs without osteogenic induction

To test the osteogenic ability of OVX-BMSCs with SrR, cultural medium without osteogenic

induction supplements were used, and qualitative ALP staining, quantitative ALP activity assay and realtime-PCR were performed.

The result of ALP assay showed that intensity of staining was stronger in 0.25 mM SrR-treated than those in other groups (Figure 3A). Quantitative ALP assay showed that SrR (0.125-2.0mM) significantly enhanced ALP activity at day 7 and 10 compared to the control group, and the ALP activity was strongest after treated with SrR at a concentration of 0.25mM at day 7 and 10 (Figure 3B).

The results of realtime-PCR demonstrated that SrR significantly up-regulated mRNA levels of Col-I, ALP, Runx2, OCN, OPG, and BSP genes those play a key role in osteogenesis process, also VEGF and ANG-1 for angiogenesis. For most of the timing and genes, 0.25, 0.5 and 1.0mM groups seemed get higher fold changes than other groups, but these three groups showed a significant decrease than control group for RANKL gene (Figure 3C).

Osteogenesis assay of OVX-BMSCs under osteogenic induction

To fully understand the osteogenic ability of OVX-BMSCs with SrR, osteogenic induction medium were also used in present study. Same as previous assay, qualitative ALP staining, quantitative ALP activity assay and Realtime-PCR were performed. What's more, alizarin red staining was conducted to analyze the mineralization ability.

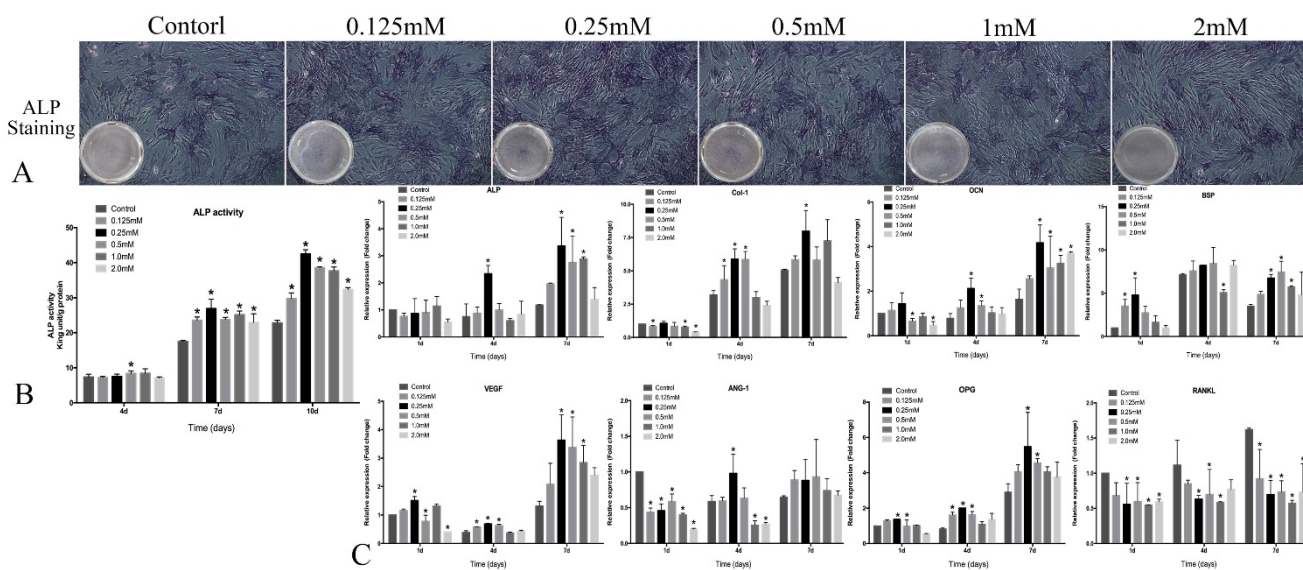


Figure 3. Osteogenesis assay of OVX-BMSCs without osteogenic induction. A, the ALP staining assay of OVX-BMSCs treated with SrR (0.125-2.0mM) for 7 days ($\times 100$); B, Quantitative assay of ALP activity at day 4, 7 and 10. C, mRNA levels of osteogenesis- and angiogenesis-related genes in the OVX-BMSCs treated with SrR (0.125-1.0mM) at day 1, 4 and 7. The experiment was repeated for at least 3 times, and the data were expressed as mean \pm SD $^*p < 0.05$ versus Control.

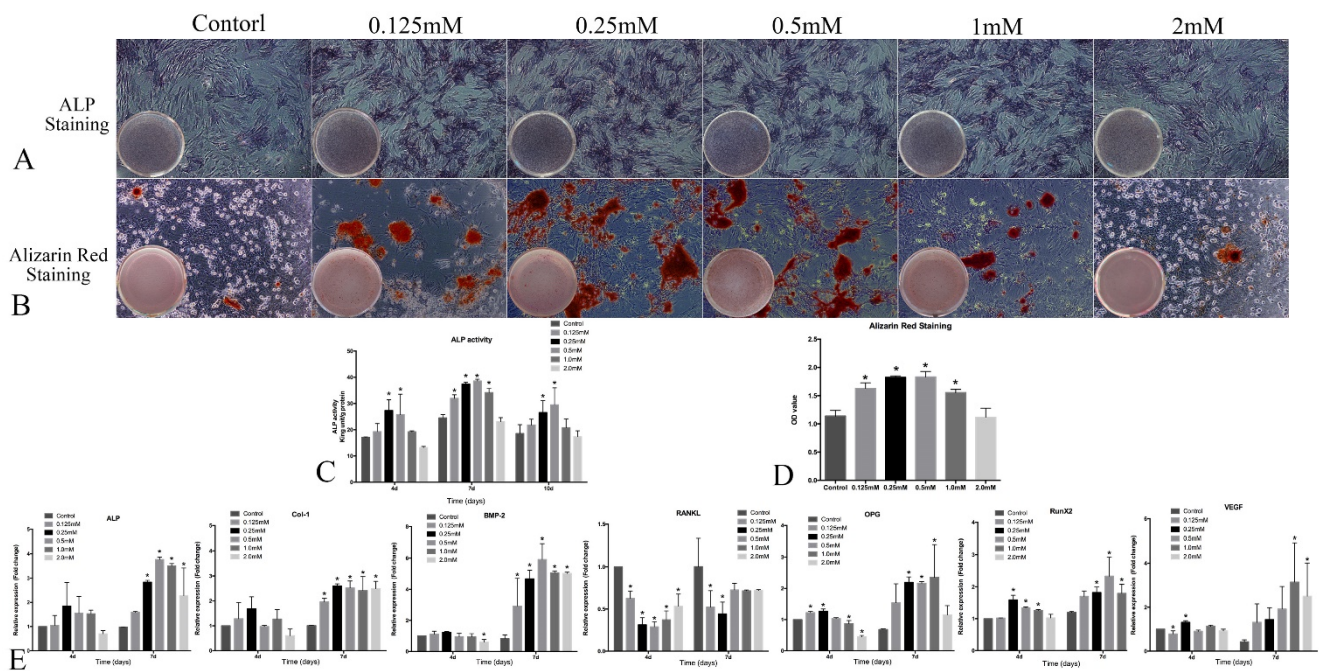


Figure 4. Osteogenesis assay of OVX-BMSCs under osteogenic induction. A, the ALP staining assay of OVX-BMSCs treated with SrR (0.125-2.0mM) in osteogenic induction cultural medium for 7 days ($\times 100$); B, Alizarin Red staining assay of OVX-BMSCs treated with SrR (0.125-2.0mM) in osteogenic induction cultural medium for 21 days ($\times 100$); C, Quantitative assay of ALP activity at day 4, 7 and 10. D, Quantitative assay of Alizarin Red Staining. E, mRNA levels of osteogenesis- and angiogenesis-related genes in the OVX-BMSCs treated with SrR(0.125-1.0mM) in osteogenic induction cultural medium at day 4, 7. The experiment was repeated for at least 3 times, and the data are expressed as mean \pm SD * $p < 0.05$ versus Control.

The intensity of ALP staining was stronger in 0.125, 0.25 and 0.5mM SrR-treated group than other groups (Figure 4A) and the same for alizarin red staining (Figure 4B and 4D). Quantitative ALP assay showed that the ALP activity at 0.25 and 0.5mM concentration of SrR were significantly higher than control group at all time points, and the whole level of ALP activity reached a peak at day 7, which was earlier than those without osteogenic induction (Figure 4C).

The results of realtime-PCR demonstrated that SrR significantly up-regulated mRNA levels of ALP, Col-1, Runx2, BMP-2, OPG and VEGF. For most of the timing and genes, SrR at 0.25- 2.0mM all showed a higher trend of fold changes than control groups, and a reduction of RANKL expression (Figure 4E).

Angiogenesis assay of OVX-BMSCs under angiogenesis induction

OVX-BMSCs under angiogenesis induction showed a behavior of tube forming after 3 days of induction (data not shown). OVX-BMSCs treated with normal cultural medium without induction or any drug performed totally lack of LDL engulfs and absence of CD31, but a low fluorescence intensity level of vWF could be observed. Those treated with induction cultural medium added with SrR showed a higher level of LDL engulf than group without SrR, and also stronger fluorescence intensity for both CD31

and vWF. While, no significant differences could be observed among the groups with 0.25, 0.5 or 1.0mM SrR (Figure 5).

Western blotting assay of OVX-BMSCs

HIF-1 α is one of the master regulators that react to hypoxia situation, which plays a crucial role in angiogenesis. The rising of HIF-1 α leads to up-regulation of VEGF and SDF-1, which act as vascular growth factors and promote cell migration for tissue injury recovery[30].

The result revealed that the protein level of HIF-1 α was highest in the OVX-BMSCs treated with SrR at a concentration of 0.25mM compared to the control, as well as VEGF and SDF-1 proteins (Figure 6).

HUVECs angiogenesis assay

The angiogenesis and thrombosis trend were evaluated by tube formation, transwell and real-time PCR assay. Obvious angiogenesis was present 6h after the incubation on Matrigel, and the HUVECs formed more branching points and loops after treated with SrR at a concentration between 0.125 and 0.5mM. Also, the transwell assay showed that the more HUVECs immigrated and crossed through the gel after treated with SrR at a concentration between 0.125 and 0.5mM (Figure 7A,B,C and D).

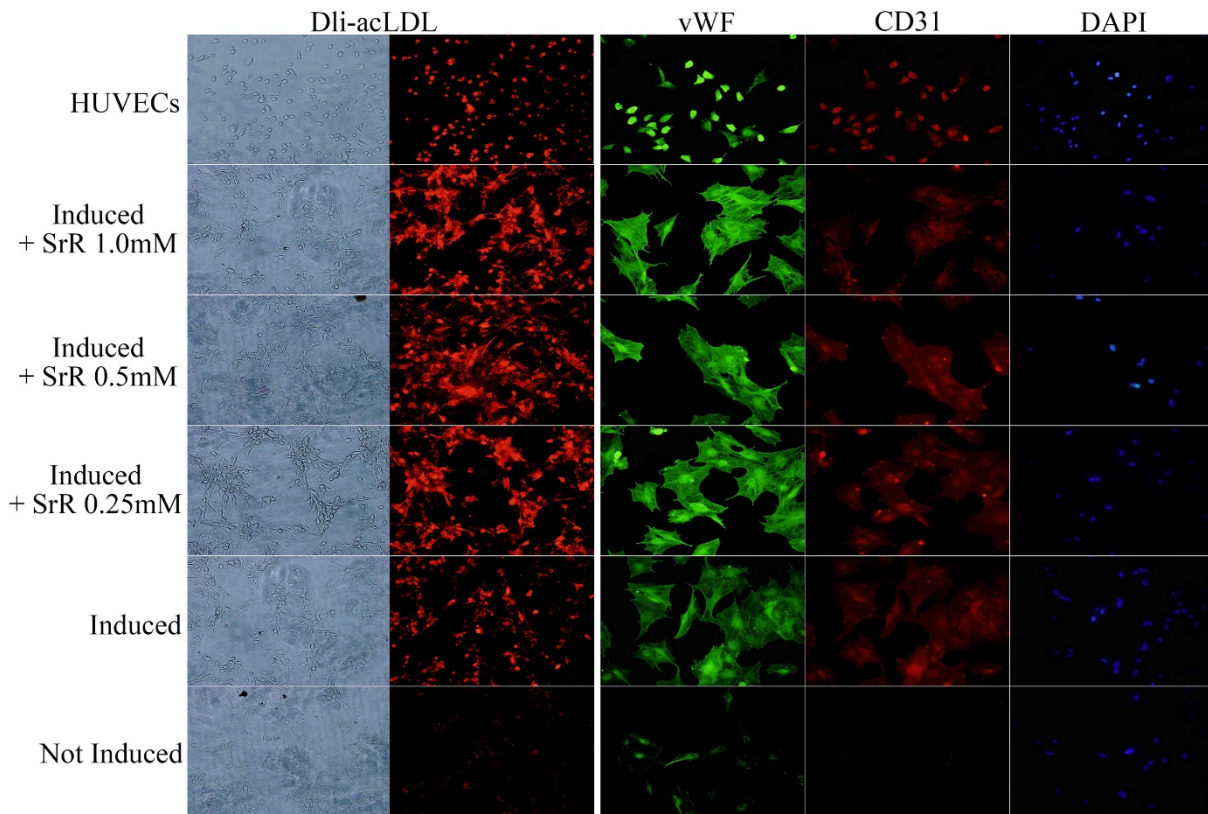


Figure 5. Angiogenesis assay of OVX-BMSCs under angiogenesis induction. The left two rows of pictures showed the Dli-acLDL uptake assay ($\times 100$), and the right three rows were the immunofluorescence staining of vWF and CD 31, DAPI showed the position of nuclei ($\times 100$).

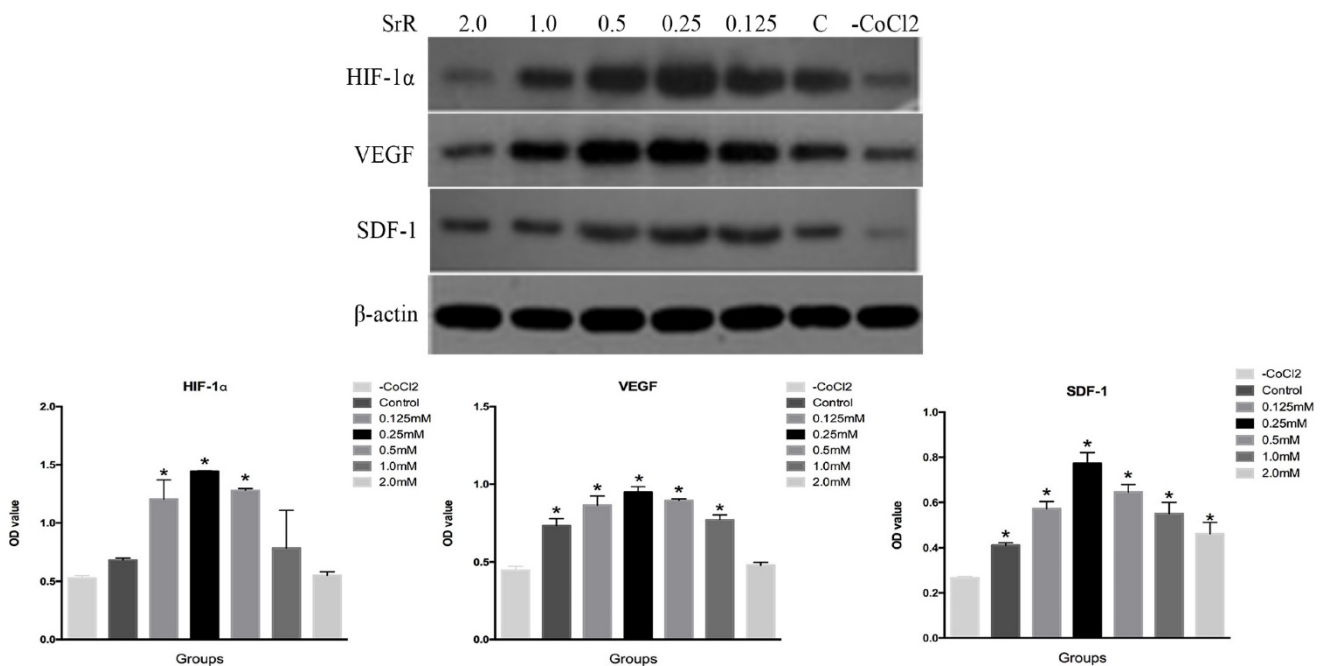


Figure 6. Western blotting assay of HIF-1 α , VEGF and SDF-1 proteins in the OVX-BMSCs treated with SrR (0.125-2.0 mM). All experiments were performed in triplicates, and the data were expressed as mean \pm SD. * $p < 0.05$ versus control.

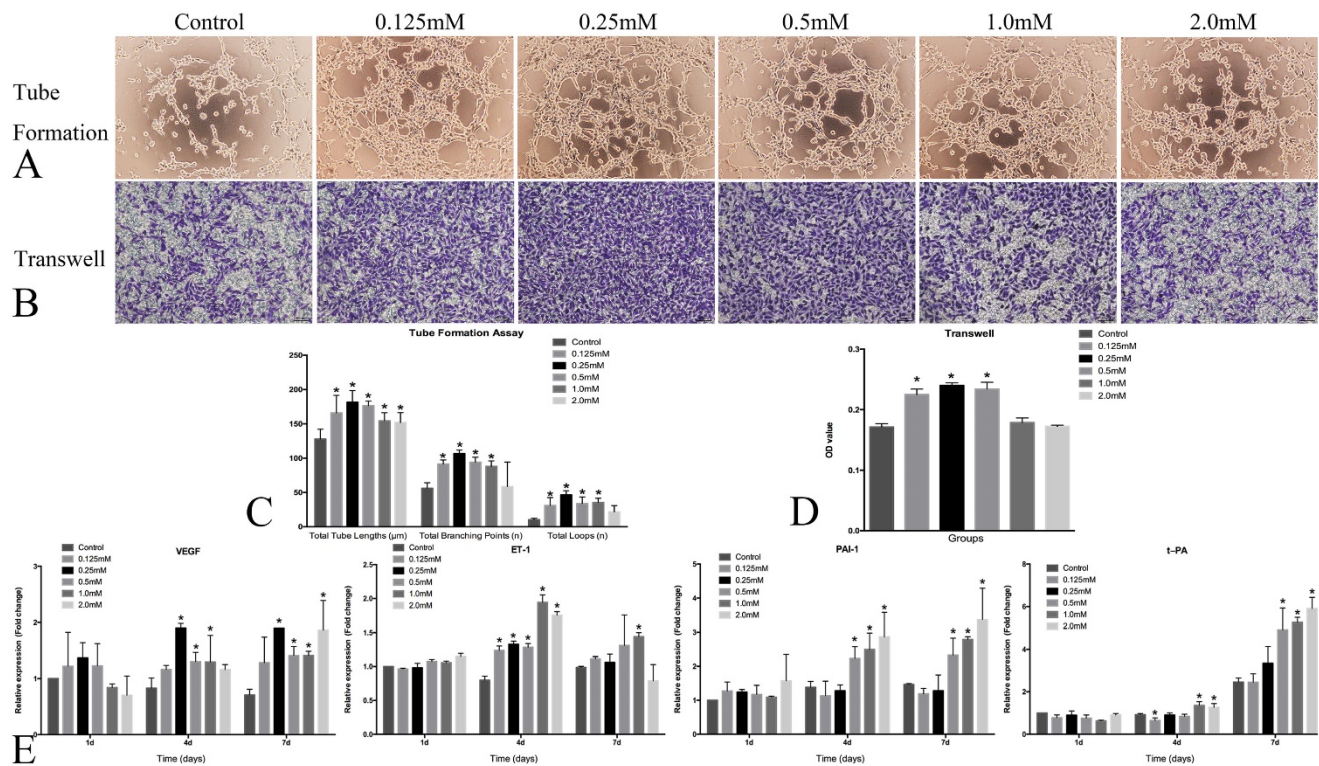


Figure 7. HUVECs angiogenesis assay. A, Tube formation assay of the HUVECs treated with SrR (0.125-2.0mM)($\times 100$); B, Transwell assay of the HUVECs treated with SrR (0.125-2.0mM)($\times 100$). All the cells passed through the transwell plates were stained in purple; C, Quantitative assay of tube formation assay, and data were expressed as mean \pm SD. * $p < 0.05$ versus Control; D, Quantitative assay of transwell. The OD value of stained crystal violet were tested and expressed as mean \pm SD. * $p < 0.05$ versus Control. E, Real-time PCR analysis of angiogenesis- and thrombosis-related genes expression in the HUVECs treated with SrR (0.125-2.0mM) at day 4, 7 and 10. Data were presented as mean \pm SD. * $p < 0.05$ versus Control.

The real-time PCR results demonstrated that SrR could significantly promote the mRNA expression of VEGF, but not ET-1 in the HUVECs at different time points. SrR (0.5-2.0mM) markedly increased PAI-1 mRNA level in the cells at day 4 and 7, and up-regulated t-PA mRNA level at day 7 (Figure 7E).

Signaling Pathway assay of HUVECs

PI3K/AKT/mTOR signaling pathway was analyzed by western blot and tubeformation assay. Western blot assay showed that AKT and mTOR were phosphorylated from as early as 15min and continued to rise (Figure 8A). To further confirm the role of PI3K/AKT/mTOR signaling pathway in SrR induced angiogenesis, PI3K/AKT inhibitor LY294002 were used. As the western blot assay shown, after inhibited by LY294002, phosphorylated AKT and p-mTOR were totally absence, while only a dim of p-mTOR could be observed if treated with SrR as well (Figure 8B). The tube forming ability of HUVECs was abolished by LY294002 (Figure 8C) that almost no loops were formed (Figure 8D).

Discussion

To the best of our knowledge, this is first time to investigate the effectiveness and safety of SrR in direct

application, especially the angiogenesis ability. The role of SrR on osteogenesis and angiogenesis of OVX-BMSCs and HUVECs were studied.

In present study, it has shown that SrR had no significant effect on the proliferation of the OVX-BMSCs at a low concentration ($< 1.0\text{mM}$), while it markedly inhibits the cell proliferation at a high concentration ($\geq 1.0\text{mM}$). Our finding is coherent to a previous study that a low dose of SrR induces the cell replication[31], but the data above 1.0mM were lack before present study.

The osteogenesis influences of SrR on OVX-BMSCs were evaluated in two ways. To clearly understand the effect of SrR, normal cultural medium was used. The result showed that SrR could directly promote osteogenic differentiation without other supplement, and the concentration between 0.25-1.0mM were high-efficiency with 0.25mM performed better. For the second assay, the osteogenic induction cultural medium was also used to learn its effect under osteogenic environment. Results were similar, 0.125-1.0mM were effective but 0.5mM were higher than 0.25mM for most of the assays. These results indicated that the concentration between 0.25-1.0mM were appropriate for direct applications and 0.25-0.5mM achieved the best effectiveness.

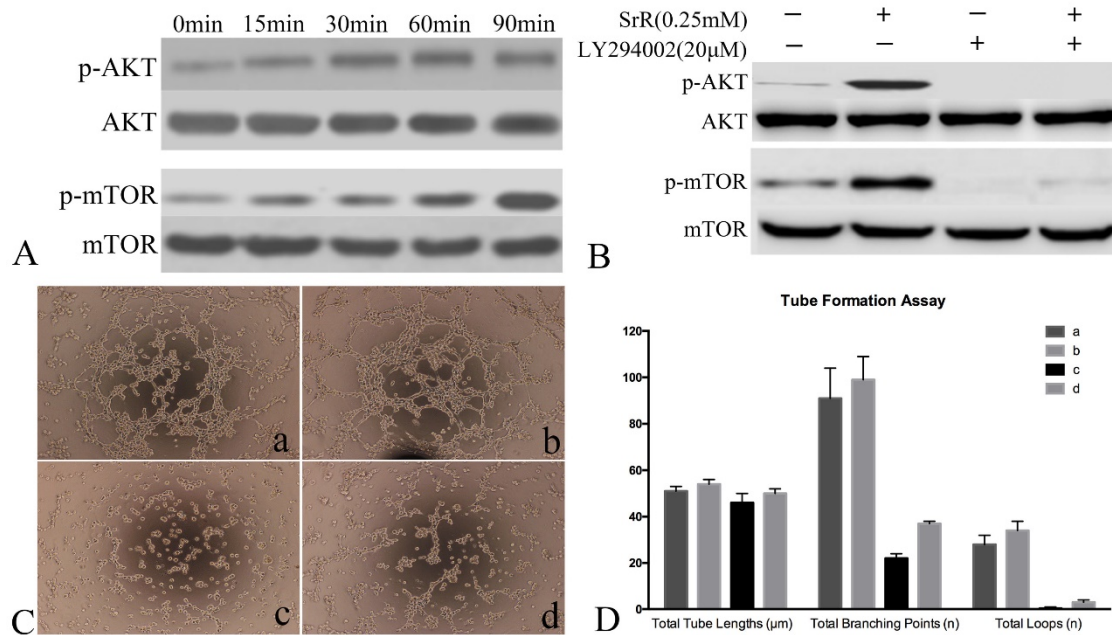


Figure 8. Signaling Pathway assay of HUVECs. A, Western Blot assay showed the protein level of AKT, p-AKT, mTOR and p-mTOR after treated with SrR at 0.25mM. A rising level of phosphorylated protein could be observed. B, Western blot assay of protein level of AKT, p-AKT, mTOR and p-mTOR with or without inhibitor LY294002 and SrR. C, Tube formation assay (a)without LY294002 or SrR; (b)without LY294002, with SrR; (c)with LY294002, without SrR; (d)with LY294002 and SrR. Magnification×100. D, The qualitative result of tube formation assay.

While, this concentration was lower than some other studies[9,11,22,31], those demonstrated that the best effect of SrR were around 1.0mM. This difference may owe to two reasons. Firstly, the method of drug treatment used in present study is different from most of the previous studies. SrR is used as a drug directly, but not the replacement of SrCl₂ and NaR. For the intact compound is different from those free ions, for example, the most obvious difference is that the intact SrR compound can only reach the highest concentration of 2.0mM in cultural medium. In addition, there is unique function for the intact SrR. SrR can antagonize NF-κB activation for osteoblast purpose, and this function can not be replaced by SrCl₂ or NaR[20], that can explain the difference results of present study with previous ones. Secondly, different cellular models or target genes may response differently to a same drug, for example, osteoblast from Calvaria cultured in osteogenic induced medium and SrCl₂ plus NaR showed a best oetogenic trend at the concentration of 1.0mM[9]; MC3T3-E1 cells cultured with SrCl₂ plus NaR performed best at the concentration of 3.0mM[15]; PA20-h5 cell line showed the best ALP activity at the concentration of 400µM[32]. The concentrations used in the previous studies also varied. Querido et al. had performed some studies using the same drug treatment method as ours, and the results were still variable[9,11,22,31,33-35]. It's reasonable that different cells with different cultural environments respond differently, so the point should not be

focused on the exact concentration, but the effective range.

The angiogenesis influences of SrR were studied by two kinds of cells. The study on OVX-BMSCs revealed that the direct application of SrR could trigger the angiogenesis induction, no matter under osteogenic induction, angiogenesis induction or normal environment. The mRNA expression of VEGF and ANG-1 were boosted after SrR treatment. Western blot assay of OVX-BMSCs showed that SrR could promote the expression of HIF-1α under hypoxia environment, which played a critical role in angiogenesis, and sequencing protein levels of VEGF and SDF-1 those vital for cell migration and revascularization were up regulated[36]. OVX-BMSCs under angiogenesis induction (cultural medium added with VEGF and bFGF) showed a significant differentiation to endothelial cells, which was more obvious with SrR treatment. Though we only performed qualitative examinations, the results gave us strong hints of its angiogenesis induction efficacy. HUVECs were standard cellular model used for learning vascular cells reaction to drugs. As can be seen from the result, SrR also has a dose-dependent effect on angiogenesis of HUVECs. The significant effects of SR on HUVECs migration and tube formation showed its high potential of angiogenesis effect. And the PCR result of VEGF showed its angiogenesis effect on RNA level, while for another marker ET-1, this drug seemed not have clear effects. As we known, there are extensive cross-talk existing

between endothelial cells and osteoblasts[37,38]. For instance, ET-1 secreted by the endothelial cells can stimulate the differentiation of osteoblast, while osteoblasts also secrete VEGF to promote the proliferation of endothelial cells conversely[39,40]. Our result showed a significant enhance of secreting VEGF of BMSCs, but no response of ET-1 from HUVECs. But things may not be true in-vivo, for we conducted this experiment by culturing cells individually, which cut down the cross talk between different cells.

The signaling pathway of PI3K/AKT/mTOR was studied on HUVECs, to understand the angiogenesis induction effects of SrR. PI3K/AKT pathway is involved in several cellular processes including cell proliferation, migration and survival, which also contribute to blood vessel formation[40]. mTOR is a key kinase downstream of this pathway, and plays a key role in angiogenesis[41]. The presenting findings demonstrated that SrR activated the phosphorylation of AKT and mTOR from 15min and continued. Combined with the result of signaling inhibits assay, it can be concluded that SrR triggered angiogenesis through PI3K/AKT/mTOR signaling pathway.

The safety of SrR direct application was evaluated by three markers related to the thrombosis effect. ET-1 is one of the most enduring and strongest endogenous vasoconstrictor peptides and a marker of endothelial dysfunction[42,43]. And combined with the result of PAI-1 and t-PA, another two markers of thrombosis, we may say that SrR at a low concentration (lower than 0.5mM) is safer for thrombosis effect. However, these results cannot be seen from single direction. Thrombosis effect will contribute to the first step of wound healing, that marked by platelet accumulation, coagulation, and leukocytes migration, to clean the infection and release growth factors[44]. This is critical procedure for tissue regeneration, so it is impossible for us to conclude that the thrombosis effect of SrR on three markers is true or dangerous for cardiovascular events. Further in-vitro or in-vivo study is needed.

Above all, the dosage between 0.25-0.5mM is more appropriate for direct application on local. While, this dosage is higher than the plasma concentration of the drug (0.12mM) that patients taking 2g SrR everyday orally after three years[21]. Our result may give some hints that locally delivery of SrR can get better benefit for local bone regeneration than orally taken method. While, further studies are necessary to evaluate the safety of local application and acquire the novel control-release of SrR.

In conclusion, SrR could promote osteogenesis and angiogenesis of OVX-BMSCs in a dose-dependent

way with 0.25-0.5mM to be more effectively. It could also enhance the angiogenesis promotion of the HUVECs, and low concentrations (<0.5mM) will not influence the gene expression of thrombosis effect. Locally application of SrR could be considered as a promising way for bone regeneration.

Abbreviations

ALP: alkaline phosphatase
 Ang-1: angiotensin-1
 bFGF: Basic fibroblast growth factor
 BMP-2: bone morphogenetic protein-2
 BSP: bone sialoprotein
 CaSR: calcium-sensing receptor
 Col-I: collagen I
 EMA: The European Medicines Agency
 European Medicine Agency
 ET-1: endothelin-1
 HIF-1 α : hypoxia inducible factor-1 α
 HUVECs: human umbilical vein endothelial cells
 OCN: osteocalcin
 OPG: osteoprotegerin
 OVX-BMSCs: ovariectomy bone marrow mesenchymal stem cells
 PAI-1: plasminogen activator inhibitor one
 RANKL: receptor activator of NF- κ B ligand
 Runx2: runt-related transcription factor 2
 SDF-1: Stromal cell-derived factor 1
 SrR: strontium ranelate
 t-PA: tissue plasminogen activator
 VEGF: vascular endothelial growth factors
 vWF: von Willebrand factor

Acknowledgements

The authors acknowledge the financial support from the Natural Science Foundation of China (81470714, 31400825, 81672134), the Science and Technology Commission of Shanghai Municipality (15410722600, 16140903900), the Advanced Research Program of Shanghai Jiao Tong University Affiliated Sixth People's Hospital (LYZY-0082, 1645), Doctorial innovation fund of medicine school of Shanghai Jiao Tong University, and Innovation fund of translational medicine of medicine school of Shanghai Jiao Tong University (15ZH2012).

Competing Interest

The authors have declared that no competing interest exists.

References

1. Curtis E M, Moon R J, Dennison E M, et al. Recent advances in the pathogenesis and treatment of osteoporosis. *Clinical Medicine*. 2015; 15 (Suppl 6):384-391.
2. Cianferotti L, D'Asta F, Brandi M L. A review on strontium ranelate long-term antifracture efficacy in the treatment of postmenopausal osteoporosis. *Therapeutic Advances in Musculoskeletal Disease*. 2013; 5(3):127-139.

3. Reginster J Y, Deroisy R, Jupsin I. Strontium ranelate: a new paradigm in the treatment of osteoporosis. *Expert Opinion on Investigational Drugs*. 2004; 13(7):857-864.
4. Reginster JY, Felsenberg D, Boonen S, Diez-Perez A, Rizzoli R et al. Effects of long-term strontium ranelate treatment on the risk of nonvertebral and vertebral fractures in postmenopausal osteoporosis: Results of a five-year, randomized, placebo-controlled trial. *Arthritis Rheum*. 2008; 58(6):1687-1695.
5. Reginster J Y, Bruyère O, Sawicki A, et al. Long-term treatment of postmenopausal osteoporosis with strontium ranelate: Results at 8 years. *Bone*. 2009; 45(6):1059-1064.
6. Reginster J Y, Bruyère O, Collette J. Strontium ranelate treatment increases osteoprotegerin serum levels in postmenopausal osteoporotic women. *Bone*. 2012; 50(5):1201-1202.
7. Seeman E, Boonen S, Borgström F, et al. Five years treatment with strontium ranelate reduces vertebral and nonvertebral fractures and increases the number and quality of remaining life-years in women over 80 years of age. *Bone*. 2009; 46(4):1038-1042.
8. Roux C, Reginster JY, Fechtenbaum J, Kolta S, Sawicki A et al. Vertebral fracture risk reduction with strontium ranelate in women with postmenopausal osteoporosis is independent of baseline risk factors. *J Bone Miner Res*. 2006; 21(4):536-542.
9. Meunier P J, Roux C, Ortolani S, et al. Effects of long-term strontium ranelate treatment on vertebral fracture risk in postmenopausal women with osteoporosis. *Osteoporosis International*. 2009; 20(10):1663-1673.
10. Bonnellye E, Chabadel A, Saltel F, et al. Dual effect of strontium ranelate: Stimulation of osteoblast differentiation and inhibition of osteoclast formation and resorption in vitro. *Bone*. 2008; 42(1):129-138.
11. Brennan T C, Rybchyn M S, Green W, et al. Osteoblasts play key roles in the mechanisms of action of strontium ranelate. *British Journal of Pharmacology*. 2009; 157(7):1291-1300.
12. Chattopadhyay N, Quinn S J, Kifor O, et al. The calcium-sensing receptor (CaR) is involved in strontium ranelate-induced osteoblast proliferation. *Biochemical Pharmacology*. 2007; 74(3):438-447.
13. Takaoka S, Yamaguchi T, Yano S, et al. The Calcium-sensing Receptor (CaR) is involved in strontium ranelate-induced osteoblast differentiation and mineralization. *Hormone & Metabolic Research*. 2010; 42(9):627-631.
14. Fromigué O, Haÿ E, Barbara A, et al. Calcium sensing receptor-dependent and receptor-independent activation of osteoblast replication and survival by strontium ranelate. *Journal of Cellular & Molecular Medicine*. 2009; 13(8B):2189-2199.
15. Fromigué O, Haÿ E, Barbara A, et al. Essential role of nuclear factor of activated T cells (NFAT)-mediated Wnt signaling in osteoblast differentiation induced by strontium ranelate. *Journal of Biological Chemistry*. 2010; 285(33):25251-25258.
16. Peng S, Zhou G, Luk K D K, et al. Strontium Promotes Osteogenic Differentiation of Mesenchymal Stem Cells Through the Ras/MAPK Signaling Pathway. *Cellular Physiology & Biochemistry*. 2009; 23(3):165-174.
17. Caverzasio J. Strontium ranelate promotes osteoblastic cell replication through at least two different mechanisms. *Bone*. 2008; 42(6):1131-1136.
18. Huizhen L, Huang X, Jin S, et al. Strontium ranelate promotes osteogenic differentiation of rat bone mesenchymal stem cells through bone morphogenetic protein-2/Smad signaling pathway. *Journal of Southern Medical University*. 2013; 33(3):376-381.
19. Atkins G, Wellton K P, Findlay D. Strontium ranelate treatment of human primary osteoblasts promotes an osteocyte-like phenotype while eliciting an osteoprotegerin response. *Osteoporosis International*. 2009; 20(4):653-664.
20. Yamaguchi M, Weitzmann M N. The intact strontium ranelate complex stimulates osteoblastogenesis and suppresses osteoclastogenesis by antagonizing NF- κ B activation. *Molecular & Cellular Biochemistry*. 2012; 359(1-2):399-407.
21. Meunier PJ; Roux C; Seeman E; Ortolani S; Badurski JE; Spector TD; Cannata J; Balogh A; Lemmel EM; Pors-Nielsen S; Rizzoli R; Genant HK; Reginster JY. The effects of strontium ranelate on the risk of vertebral fracture in women with postmenopausal osteoporosis. *New England Journal of Medicine*. 2004; 350(5):459-468.
22. Verberckmoes S C, Broe M E D, D'Haese P C. Dose-dependent effects of strontium on osteoblast function and mineralization. *Kidney International*. 2003; 64(2):534-543.
23. Breart G, Cooper C, Meyer O, et al. Osteoporosis and venous thromboembolism: a retrospective cohort study in the UK General Practice Research Database. *Osteoporosis International*. 2010; 21(7):1181-1187.
24. Reginster J Y. Cardiac concerns associated with strontium ranelate. *Expert Opinion on Drug Safety*. 2014; 13(9):1-5.
25. Tsolaki I N, Madianos P N, Vrotsos J A. Outcomes of Dental Implants in Osteoporotic Patients. A Literature Review. *Journal of Prosthodontics Official Journal of the American College of Prosthodontists*. 2009; 18(4):309-323.
26. Tian A, Zhai J J, Peng Y, et al. Osteoblast response to titanium surfaces coated with strontium ranelate-loaded chitosan film. *International Journal of Oral & Maxillofacial Implants*. 2014; 135(29):1446-1453.
27. Nair B P, Sindhu M, Nair P D. Polycaprolactone-laponite composite scaffold releasing strontium ranelate for bone tissue engineering applications. *Colloids & Surfaces B Biointerfaces*. 2016; 143:423-430.
28. Shen Q, Zeng D, Zhou Y, et al. Curculigoside promotes osteogenic differentiation of bone marrow stromal cells from ovariectomized rats. *Journal of Pharmacy & Pharmacology*. 2013; 65(7):1005-1013.
29. Dominici M, Blanc K L, Mueller I, et al. Minimal criteria for defining multipotent mesenchymal stromal cells. The International Society for Cellular Therapy position statement. *Cytotherapy*. 2006; 8(4):315-317.
30. Mirshahi F, Pourtau J, Li H, et al. SDF-1 activity on microvascular endothelial cells: consequences on angiogenesis in in vitro and in vivo models. *Thrombosis Research*. 2000; 99(6):587-594.
31. Li Y, Li J, Zhu S, et al. Effects of strontium on proliferation and differentiation of rat bone marrow mesenchymal stem cells. *Biochemical & Biophysical Research Communications*. 2012; 418(4):725-730.
32. Nardone V, Zonefrati R, Mavilia C, et al. In Vitro Effects of Strontium on Proliferation and Osteoinduction of Human Preadipocytes. *Stem Cell International*. 2015; 2015(5):1-12.
33. Zhu L L, Zaidi S, Peng Y, et al. Induction of a program gene expression during osteoblast differentiation with strontium ranelate. *Biochemical & Biophysical Research Communications*. 2007; 355(2):307-311.
34. Querido W, Farina M. Strontium ranelate increases the formation of bone-like mineralized nodules in osteoblast cell cultures and leads to Sr incorporation into the intact nodules. *Cell & Tissue Research*. 2013; 354(2):573-580.
35. Querido W, Campos A P, Martins Ferreira E H, et al. Strontium ranelate changes the composition and crystal structure of the biological bone-like apatite produced in osteoblast cell cultures. *Cell & Tissue Research*. 2014; 357(3):793-801.
36. Villars F, Guillotin B, Amédée T, et al. Effect of HUVEC on human osteoprogenitor cell differentiation needs heterotypic gap junction communication. *Ajp Cell Physiology*. 2002; 282(4):C775-C785.
37. Clarkin C E, Emery R J, Pitsillides A A, et al. Evaluation of VEGF-mediated signaling in primary human cells reveals a paracrine action for VEGF in osteoblast-mediated crosstalk to endothelial cells. *J Cell Physiol. Journal of Cellular Physiology*. 2008; 214(2):537-544.
38. Wang D S, Miura M, Demura H, et al. Anabolic effects of 1,25-dihydroxyvitamin D-3 on osteoblasts are enhanced by vascular endothelial growth factor produced by osteoblasts and by growth factors produced by endothelial cells. *Endocrinology*. 1997; 138(7):2953-2962.
39. Qin L, Qiu P, Wang L, et al. Gene expression profiles and transcription factors involved in parathyroid hormone signaling in osteoblasts revealed by microarray and bioinformatics. *Journal of Biological Chemistry*. 2003; 278(22):19723-19731.
40. Bader A G, Kang S, Zhao L, et al. Oncogenic PI3K deregulates transcription and translation. *Nature Reviews Cancer*. 2005; 5(12): 921-929.
41. Karar J, Maity A. PI3K/AKT/mTOR pathway in angiogenesis. *Frontiers in molecular neuroscience*. 2011; 4: 51.
42. Arai H, Hori S, Aramori I, et al. Cloning and expression of a cDNA encoding an endothelin receptor. *Nature*. 1990; 348(6303):730-732.
43. Ziv I, Fleming G, Djaldetti R, et al. Increased plasma endothelin-1 in acute ischemic stroke. *Stroke; a journal of cerebral circulation*. 1992; 23(7):1014-1016.
44. Kirsner R S, Eaglstein W H. The wound healing process. *Dermatologic Clinics*. 1993; 11(4):629-640.